Morphotectonic Expressions of the Drainage Basins and Channel Long Profile Forms on a Selected Part of Sikkim-Bhutan Himalayas

Ujwal Deep Saha (ID)**, Nilanjana Biswas** (ID)**, Sushonova Mondal** (ID)**, and Soma Bhattacharya** (ID)

Abstract This study is an endeavour for analysing the neotectonic signatures reflected at basin scale for few selected rivers in the eastern part of Himalayas through the application of morphotectonic indices. River catchments around the Jaldhaka re-entrant have been considered in this study due to its proven sensitivity to neotectonic perturbations. Since, the impact of neotectonics has already been sensed on the pied-mont segment, the nature of sensitiveness of the fluvial forms at the entire catchment scale to tectonic deformations has been the focal theme of this study. The selection of the eleven morphotectonic indices was done pondering on three major geomorphic perspectives; basin form components, basin and valley relief components and channel long profile form parameters. The nature of the geomorphic signatures found at the basin scale, river valleys and along the river courses have steered towards an ongoing adjustment of the fluvial units with active tectonism. Invariably the catchments are experiencing a state of dynamic equilibrium where adjustment between the fluvial activity and tectonic upliftment along the major thrusts is characteristic of fluvial form modifications within the studied catchments. The neotectonic perturbations have its indentations reflected in the channel long profile form adjustments with characteristic differences of channel responses related to different expressions of surface warping. Spatial associations of the knick points has been observed in a close correspondence with the Himalayan thrusts and surface deformations, developed on the alluvial reaches of the foredeep plain are explicitly associated with the neotectonic twitching.

Keywords Drainage basin · Himalayas · Morphotectonics · Neotectonics · Long profiles

U. D. Saha
University of Calcutta, Kolkata 700073, India

N. Biswas (✉)
Vivekananda College for Women, Kolkata 700008, India

S. Mondal
SACT-I, Surendranath College for Women, Kolkata 700009, India

S. Bhattacharya
Vivekananda College for Women, Kolkata 700008, India

1   Introduction

Probing the geomorphological parameters of river catchments helps to analyse the modification of surface forms where alongside with different other factors, tectonics plays an important part (Holbrook and Schumm 1999). The morphotectonic indices have been proven to be a useful tool to extract the geomorphic expressions developed due to the tectonic impact at various geomorphic tiers within a river catchment (Keller and Pinter 1996). It helps to disclose the nature of continuous competition between the tectonic processes responsible for developing the topographical expressions and the surficial process that tends to modify the surface expressions (Burbank and Anderson 2012). The resultant effects of being tectonically sensitive are immediately reflected in catchment morphometry as well as channel forms. It is because the settings of regional tectonic features or local impact of surface deformations control the evolution process of the fluvial systems that traversing through (Schumm 1986). The basin shape perspective, terrain morphological expressions as well as the evolution stages of the fluvial system along with the long profile form adjustment are characteristically governed by the regional tectonic disposition (Bull and Mcfadden 1977; Cox 1994; Keller and Pinter 2002; Bull 2007). The most suitable spatial extent to apply these indices have been proved to be at the mountainous terrain with associated flat tracts experiencing an ongoing competition between the surface processes and underlying geometry of the active orogens at a catchment level (Bull 2007; Figueiredo et al. 2017; Flores-Prieto et al. 2015; Moussi et al. 2018; Altm 2012; Kashani et al. 2009).

Considering the above-mentioned attributes, the Himalayas are the first place that could strike first within the Indian sub-continent to apply the morphotectonic approach for extracting the signatures of the Quaternary tectonics. The ongoing development of the Himalayas due to the continuous submergence of the Indian plate at a differential rate over the period has been responsible for being pierced with tectonic wrapping and deformations during the Quaternary period (Valdiya 2002). It has resulted in controlling the fluvial systems both at catchment and fluvial scale (Nakata 1989; Valdiya et al. 1984; Valdiya 1986; Lave and Avouac 2000; Kumar and Thakur 2007). In the past couple of decades, several attempts have been conducted to study the tectonic imprints on the Himalayan terrain and its associated forelands using geomorphic indices. Whereas, the North-Western Himalayas has been at the foci of the majority of the initiatives (Sharma et al. 2017; Joshi et al. 2016; Bali et al. 2016; Chatterjee et al. 2019; Goswami and Pant 2008; Kaushal et al. 2017; Malik and Mohanty 2007; Philip and Suresh 2009; Dube and Satyam 2018; Pant and Singh 2017; Phartiyal and Kothyari 2011; Sharma et al. 2017; Singh and Tandon 2008; Virdi et al. 2007). In the recent past, the nature of surface deformations and markers of active tectonism in certain pockets of the Sub-Himalayan part of the Sikkim- Bhutan Himalayas have been attempted to study in detail (Goswami et al. 2012; Guha et al. 2007; Chakraborty and Mukhopadhyay 2013; Kar and Chakraborty 2014; Mukul et al. 2014; Ayaz et al. 2018) but not a single attempt was made to analyse the spatiality of channel responses at catchment tier to active tectonism on a continuous

stretch over this region. Although, the Jaldhaka re-entrant has been talked for its tectonic sensitiveness (Nakata 1972) and above-mentioned works were conducted to identify the tectonic activeness of the rivers mostly on the piedmont plain or mountain-piedmont juncture but not a single efforts being made to characterise the overall catchment scale sensitiveness of the rivers around this region in accumulation. Ayaz and Dhali (2019) had made an effort to analyse the longitudinal characteristics of a few of the rivers selected in this study but no significant relation being shown between the structural elements and relative channel longitudinal form adjustment. Thus, a significant research gap persists within this region in terms of an overall relationship between the Himalayan tectonic perturbations and adjustment of both the channel longitudinal form and catchment character.

In this study, neotectonic sensitiveness of the river catchments on a particular segment of the Eastern Himalayan has been tried to study using selected morpho-tectonic indices, efficient at river catchment scale and the resultant form adjustment of the fluvial systems were adhered by analysing the long profile forms of selected rivers. The regionality of the resultant surface warping due to tectonic impacts and its resultant effects as portrayed in the evolution and form adjustment of the fluvial system, located on a certain part of the Eastern Himalayas has been the focal theme of this work. The shape perspective of the catchment, the competition for dominance between tectonic disquiets and fluvial activity along the mountain front, the relief differentiation at the catchments and the responsive overall channel form were analysed in this study using the concerned geomorphic indices. The regional distribution of certain breaks in the river longitudinal profile as a resultant expression of differential upliftment of and along the mountain fronts, marked using relative slope extension method was considered as the portrayal of the direct response of the rivers to the active tectonism.

2 Study Area

This study deals with eleven selected river catchments located around the Jaldhaka re-entrant. All of these have been originated on the Sikkim-Bhutan Himalayas and drained two major physiographic regions in the eastern part of the Himalayas; i.e. Himalayan crystalline terrain and the associated piedmont surface (Fig. 1).

The Himalayan thrust loading during the process of Himalayan formation has given rise to prominent topographic regions and structural hegemonies over this area (Burbank et al. 1996). The Himalayan thrusts have separated the certain age-specific structural segments of the Himalayas into the specific tectono-geomorphic region along with the outflanking foredeep basin that occurred due to the flexural down buckling along the tertiary depo-centre called the Siwaliks (Yin 2006) (Table 1). Since the convergence between the Asian and Indian plates continues, the development of these tectono-geomorphic regions is still active and hence tectonically sensitive. The Main Boundary thrust has separated the crystalline lesser Himalayan succession from the Tertiary foreland basin succession. The foreland basin succession is partly
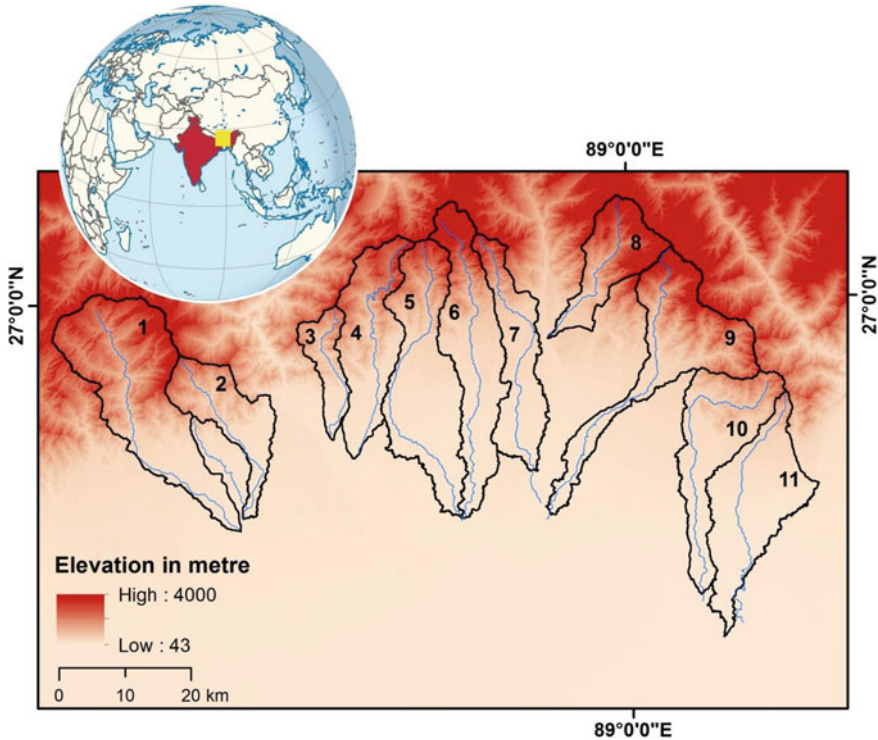
Fig. 1 Location of the study area

composed of the Neogene sedimentary succession called Siwalik (Chakraborty et al. 2020) (Fig. 2). The Himalayan Frontal Thrust has separated this fossiliferous sedimentary formation from the peripheral Quaternary sediment fill basin of the foreland depo region called the foredeep plains. The presence of the Siwalik formation is not continuous in the study area rather, certain gaps persist with the exposure of crystalline middle Himalayan succession to the Quaternary sediments, called the Siwalik Gap (Mallet 1875) (Fig. 3). These gaps were formed due to either the Siwalik being masked out by the Quaternary sediments and eventually the MBT has overridden it or due to lack of lithification that led to the absence of Siwalik formation (Gansser 1964). It has led to the presence of the crustal shortening with widespread sediment depositions called the Himalayan Reentrants (Dasgupta et al. 2013). The study area has been considered based on a prominent reentrant, the Jaldhaka Reentrant, designated by Nakata (1972). Channels originated on the mountain terrain and developed its courses around the axial part of the reentrants before entering the foredeep plain have been considered in this study. Broadly, this study area can be divided into four physiographic regions; the crystalline and sedimentary Himalayan Front or the lithified region, the Bhabar region with rock fragments and Quaternary valley-fill
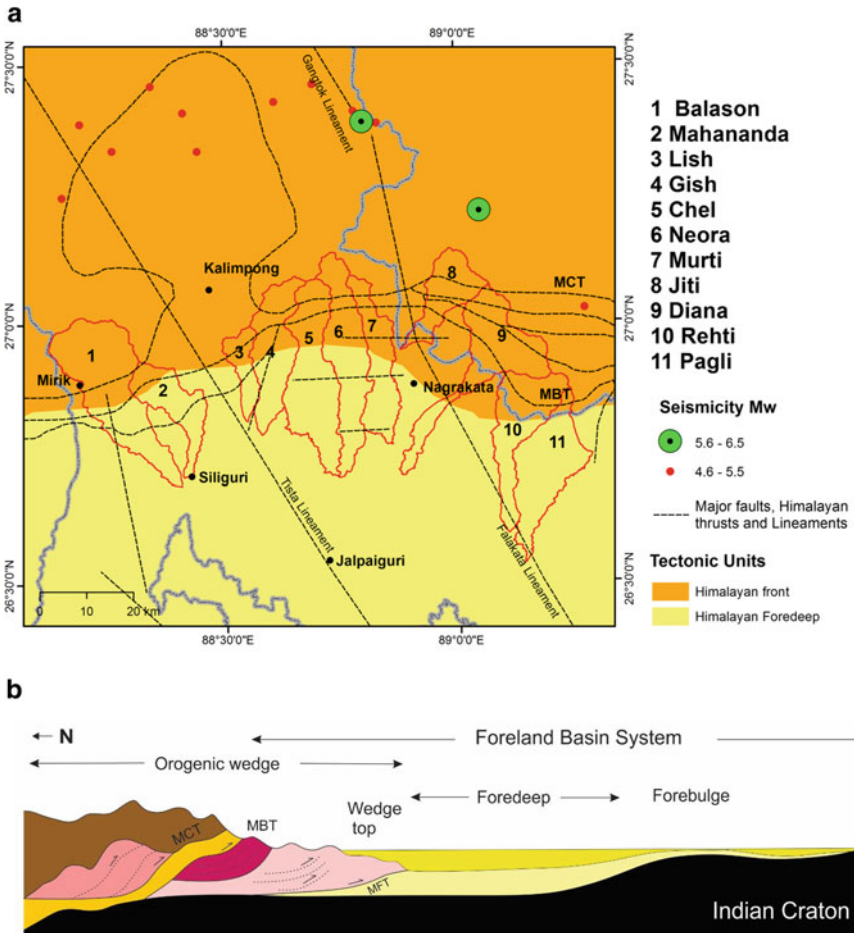
Fig. 2 **a** Structure and tectonic elements of the study area **b** Stratigraphic profile across the Himalayan belt and associated foreland (after DeCelles and Giles 1996)

deposits, the Terai region with moist alluvium, and the low lying alluvial plains with finer sediments (Chattopadhyay and Das 1979).

The Himalayan thrusts have impinged the development of the multiple thrust parallel faults on the Himalayan terrain while the Quaternary period has experienced reactivation of multiple thrust parallel and NNW-SSE oriented fault lines on the foreland segment. Thrust parallel topographic ridges with respective elevation drop towards the south, the south-dipping scarps, intraformational thrust faults and the river gorges are the characteristic tectono-geomorphic features on the orogenic wedge of the Himalayas. On the other hand, the association of blind thrusts, flexural deformations and uplifted sedimentary basins, south flanking scarps associated with
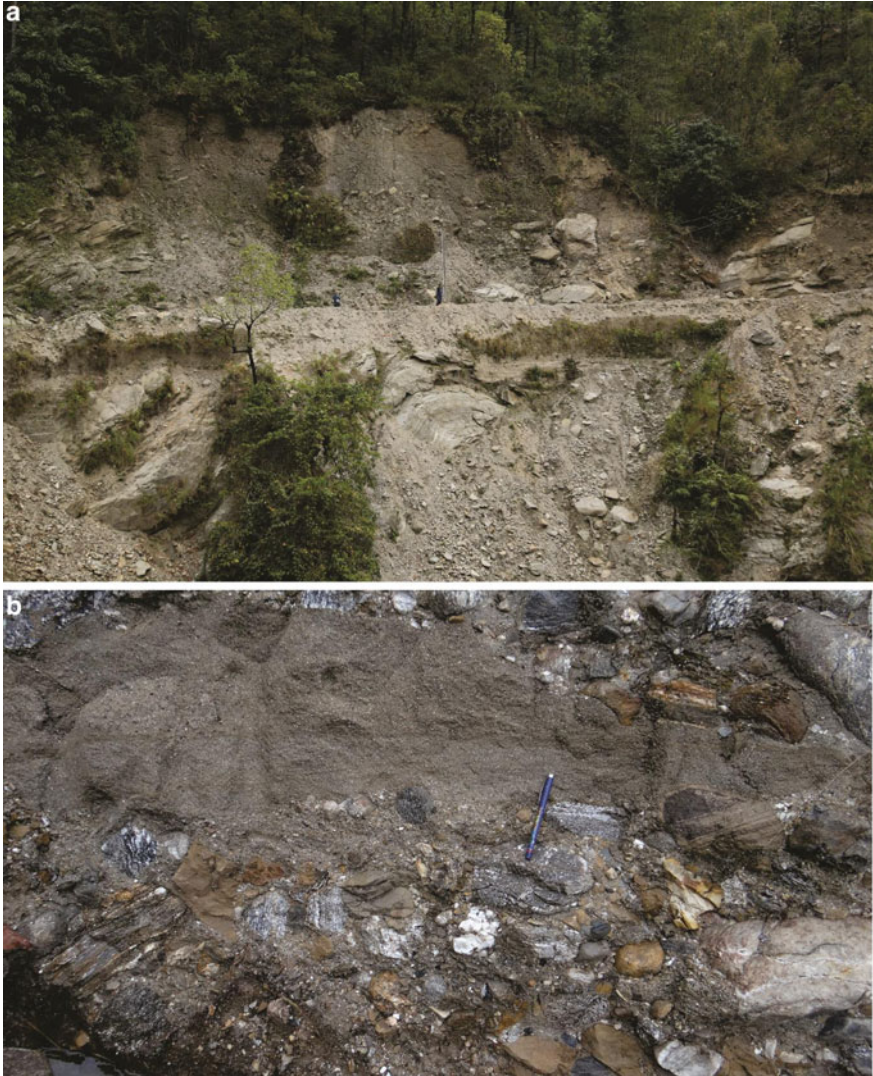
Fig. 3 **a** Quaternary fan deposits above the Middle Himalayan crystalline formation (Siwalik gap region) found at the mountain front in the Chel river basin; **b** Siwalik formation (conglomerate) with interbedded sand (Pliestocene fan deposits) found around the mountain-piedmont part of Murti River; DOC: a. 14.3.2019, b. 18.2.2017

the MBT and MFT along with the fault parallel drainage systems have been developed on the foredeep sedimentary basin in the study area (Starkel et al. 2008; Nakata 1972, 1989; Chattopadhyay and Das 1979).

3   Materials and Methods

In this study, the selected eleven drainage basins originated on the Himalayan complex have been studied for the required spatial properties of speckled dimensions. Shuttle Radar Topographic Mission (SRTM) Dem of 30 m and Landsat 8 images captured in 2019 were used for acquiring the elevation properties and concerned spatial parameters, both linear and areal respectively.

3.1   Pre-processing of the Data Used and Application of Dem

Correcting the radiometric property of Digital Elevation Model (DEM) and reducing its' elevation error are the essential practices before extracting spatial data from it (Hawker et al. 2018). The radiometry of the dem was corrected by removing the noises from the database using the smoothing technique in Geomatica v12. The radiometry of the dem was required to be corrected for lowering down the RMSE (Root Mean Squared Error). It was performed here by cross-referencing it with 235 ground control points taken from the bare part of the region to outcast the vegetation sensitivity of SRTM DEM. Before comparing the two point clouds, the Toposheet was resampled to WGS 84 datum. The RMSE of the prepared dem at z-direction lies at 0.52 m. Arc-Gis watershed module was used to delineate the basins, located around the Jaldhaka re-entrant. The void points found in the mosaicked dem surface were corrected by using the DEM Fill property in the Hydrology module. To delineate the drainage network, it was approximated by using the D8 algorithm where the flow direction was traced down by the flow away from each pixel to its 8 neighbourhood pixels. The DEM-derived drainage networks were furthered corrected using the Landsat 5 image acquired in 2000. Since the Dem determines the steepest possible path, sometimes it doesn't correspond to the actual river path on the plains. The use of satellite images acquired in 2000 has helped to identify the actual extensions of the channels on the piedmont and also in masking out the vegetation sensitiveness of the C band used in SRTM data.

3.2   Morphotectonic Indices

The morphotectonic approach has been a globally putative stream of analyzing the overall control of tectonics at the basin scale (Phartiyal and Kothyari 2011; Partabian et al. 2016; Sharma and Sarma 2017; Ghosh and Shivakumar 2018; Moussi et al. 2018). In this study, the morpho-tectonic indices were selected based on three major dimension perspectives of the basin. For analyzing the basin shape, Basin shape factor (Bs), Form factor (Bf), Circularity ratio (Cr) and Elongation ratio (Re) was considered. To study the asymmetry perspective of the basin or basin tilt, Topographic

Symmetry Factor (TTSF) has been calculated. In the case for analyzing the basin topographic extremities, Relief ratio (Rr), Topographic Roughness Index (STD) and Hypsometric integral (HI) were computed (Table 1). The linearity and the relative fluvial dominance over the orogenic processes, the Valley floor width to valley height ratio (Vf) and Mountain front sinuosity (Mfs) were calculated. The indices have been elaborated in Table 1. A general understanding of basic geometric and altitude characteristics of the selected basins has been elaborated in Table 2.

3.3 *River Longitudinal Profile and Related Indices*

The longitudinal profile of a river represents a curve depicting the gradient of the valley with corresponding distances from the source to the mouth. It portrays the geomorphic history of a river basin (Sen 1993; Sinha and Parker 1996; Jain and Sinha 2006; Chen et al. 2006). The channel long profile has been crammed by many researchers to extract the tectonic upshots both at the basin scale and floodplain level (Hack 1957; McKeown et al. 1988; Lee and Tsai 2010; Seeber and Gornitz 1981; Lu and Shang 2015; Kale et al. 2013; Moussi et al. 2018). The form of long profiles has been studied using different indices to depict its nature and relative anomalies. The long profiles of the eleven selected rivers were extracted from the DEM after compartmentalising the path into 50 m segments and the downstream points of each segment were converted into a point vector. The x, y and z values of the point vector were converted into a file format that is suitable for MS Excel ('.csv' file format was used). The distances between the points were calculated using the Eq. 1

$$d = \sqrt{\left\{(x_2 - x_1)^2 + (y_2 - y_1)^2\right\}} \tag{1}$$

where, d = distance between points X1 and X2, X1 = X—coordinate (in meters) of point X1, Y1 = Y-coordinate (in meters) of point Y1, X2 = X-coordinate of point X2, Y2 = Y-coordinate of point Y2.

3.3.1 Mathematical Models

Curve fitting is one of the most common practices to evaluate the formation of river longitudinal profile. It can be a simple linear, logarithmic, exponential and, power regression models that feature a picture of ongoing processes. The Sum of Squared Errors (SSE) and the Coefficient of determination (R^2) determine the model's best fit with the curve (Lee and Tsai 2010).

$$\text{The Linear function y} = ax + b \tag{2}$$

Table 1 Maps and images used in the study

Properties	Index	Mathematical derivation	Explanations	Source
Basin form and symmetry	Shape factor	L/B Where L = Basin Length, B = Basin Width	Higher values indicate elongation whereas lower values indicate oval and round-shape catchments	After R.E. Horton (1932)
	Form factor (F_f)	$F_f = A/L^2$ Where A = Basin Area, L = Basin Length	Higher values indicate bulging and oval-shaped basin whereas lower values indicate elongated basin	After R.E. Horton (1932)
	Circularity Ratio (C_R)	$C_R = 4\pi A/P^2$ Where A = Basin Area, P = Area of a circle with same basin perimeter	$C_R > 1$; circular form $C_R < 1$; elongated or oval-shaped form	After Miller (1953)
	Elongation ratio (R_e)	$R_e = (2\sqrt{A/\pi})/L_b$ Where, A = Basin area, L_b = Maximum Length of the Basin	$R_e < 0.50$; tectonically active $R_e = 0.50$ to 0.70; slightly active $R_e > 0.70$; tectonically inactive	Bull and McFadden (1977)
	Topographic symmetry factor (T)	T = Da/Dd Da is the distance from the channel to the basin midline. Dd is the distance from the lateral basin margin to the basin midline	T = 0; symmetric basin with no ambiguities T > 0 asymmetric basin	Cox (1994)
Basin relief	Relative relief (H)	H = (H/P) × 100 Where H = Difference between highest and lowest point, P = Perimeter	Determine the degree of dissection	M.A. Melton (1957)
	Relief ratio (R_f)	$R_f = (E_{max} - E_{min})/L_b$ Where E_{max} Maximum = elevation of the basin, E_{min} = Minimum elevation of the basin, L_b = Longest length of the basin	High values of relief ratio indicate steep slope and high relief. In other side low values indicate small ridge with lower degree of slope	Panek (2004)

Table 1 (continued)

Properties	Index	Mathematical derivation	Explanations	Source
	Topographic roughness index (STD)	Standard deviation of the elevation value	Magnitude of topographic variability; higher the value greater is the roughness	Klinkenberg (1992)
	Hypsometric integral (HI)	$HI = (H_{mean} - H_{min}) / (H_{max} - H_{min})$ Where H_{mean} = Average of elevation, H_{max} & H_{min} = Maximum and Minimum elevation of area respectively	$HI > 0.6$ characterise tectonic mobility $HI < 0.6$ indicates mature stage of development	Strahler (1952)
Mountain front	Mountain front Sinuosity (Mfs)	$Smf = (L_{mf}/L_s)$ Where L_{mf} = Length along the edge of the mountain piedmont junction, L_s = Overall length of the mountain front	$Smf < 1.4$ tectonically active areas $Smf = 1.4$–3 slightly active areas $Smf > 3$ inactive areas	Bull and McFadden (1977)
	Valley width to height ratio (Vf)	$Vf = 2V_{fw}/\{(E_{ld}-E_{sc}) + (E_{rd}-E_{sc})\}$ Where, V_{fw} = width of the valley floor, E_{ld} & E_{rd} = Elevation of left and right valley divides respectively, E_{sc} = Elevation of valley floor	$Vf < 1$ characterise active incision $Vf >$ active deposition into a broad valley	Bull and McFadden (1977)

$$\text{The Exponential function } y = ae^{bx} \tag{3}$$

$$\text{The Logarithmic function } y = a \ln x + b \tag{4}$$

$$\text{The power regression model } y = ax^b \tag{5}$$

Here, y stands for elevation and x is for length. The mathematical models of curve fitting are based on the relationship between the grain sizes of sediments with channel capacity. When the channel bed grain size is greater than the transportation capacity of the river, the long profile shows a low degree of concavity and best fit by linear function curve. If the deposition and transportation of a stream experiences a dynamic equilibrium state, the long profile would fit the exponential function. Whenever the profile is subjected to follow a graded shape, the sediment size of the stream would decrease downstream, and the logarithmic function would be the best fit. With the

Table 2 Linear and relief properties of the trunk stream and the catchments

Catchments	Basin area	Basin length	Basin perimeter	Width	Maximum elevation	Mean elevation	Minimum elevation	Relative relief	Length of the trunk stream
Balason	392.953	42.054	122.749	17.473	2614	1351.56	110	2504	42.05
Mahananda	157.199	26.701	84.738	9.641	2233	1168.72	133	2010	26.70
Lish	78.933	20.386	54.729	8.36	1887	984.47	116	1771	20.38
Gish	221.663	34.524	94.593	11.159	2359	1214.37	115	2244	34.52
Neora	324.683	42.343	132.833	12.795	3160	1624.51	94	3066	47.92
Chel	281.502	47.926	139.36	9.987	2464	1262.56	94	2370	42.34
Murti	188.542	37.015	110.933	8.395	2537	1295.57	105	2432	37.01
Jiti	149.302	24.44	74.249	11.902	3461	1805.89	231	3230	24.44
Diana	247.937	39.422	139.47	23.124	2546	1317.13	95	2451	39.42
Rehti	235.366	34.746	107.419	14.057	1820	903.63	64	1756	34.74
Pagli	270.063	38.187	115.328	17.17	1619	818.88	60	1559	38.18

additional rate of increase in concavity, the power function is most suitable (Lee and Tsai 2010).

3.3.2 Stream Length Gradient Index (SL)

The stream length gradient index is a parameter that evaluates the erosional resistance of the rocks and the relative intensity of tectonic activity (Rhea 1993). The SL index was proposed by Hack (1973) related to the hydrographic network and slopes of the river channel, is the function of the power of the stream per unit length and as a proportion to the total stream power available at a particular river reach (Summerfield 1991; Pérez-Peña et al. 2010). It is expressed as follows

$$SL = (\Delta H/\Delta L) \times L \qquad (6)$$

where ΔH is the elevation change, ΔL is the horizontal length for a given channel reach, and L is the horizontal distance from the midpoint of the reach to the drainage divide (Fig. 4).

It can be obtained also from the semi-logarithmic form of the longitudinal profile, where gradient index is equal to the constant K, the slope of the profile and can be expressed as

$$K = (h1 - h2)/[\ln(d2) - (d1)] \qquad (7)$$

where h is the elevation and d is the distance, 1 and 2 are the successive points.

The ratio of average SL value and the k of a certain river was proposed by Seeber and Gornitz (1981) as the Normalized Stream Gradient Index (NSL). It was considered by Lee and Tsai (2010) as the Channel Steepness Index that displays the rate of fluvial erosional process of a river. The values of NSL ≥ 2 indicate significantly
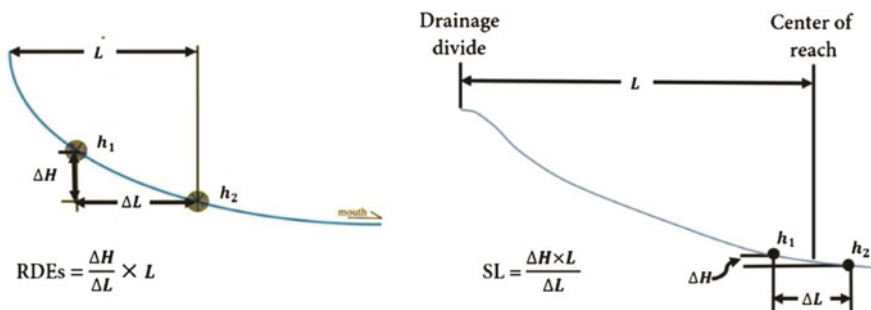

Fig. 4 Schematic scetch of the method used to calculate SL and Rdet (after Moussi et al. 2018)

steeper reaches whereas NSL $\geq$ 10 is classified as highly steep reaches. The NSL index explains the instability of a particular area.

3.3.3 Relative Slope Extension Index (RDEt)

RDE index is an indicator that implies the relation between stream discharge energy and slope of a river channel. Etchebehere et al. in 2004 prepared the RDE index as derivatives of the SL index (Hack 1973). It is regarded as a useful tool to identify knick points in a river long profile (Moussi et al. 2018). The total RDE index refers to the total length of the river and the total slope of the channel with the logarithm of total channel length.

$$RDEt = (\Delta H/\Delta L) \times \ln (L) \qquad (8)$$

where ΔH is the elevation difference between the extremes of given stream reach, ΔL is the length of the segment, and quantity and L is the stream length.

The existence of Knick points in the long profile demarcates the influence of tectonics and lithology on the development of river characteristics. The Knick points are identified by filtering of RDE index values and the interpolation of Knick points was done by using the RDEt values.

4 Neotectonic Movements and Channel Evolution

4.1 Morphotectonic Characteristics of Different Geomorphic Tiers; River Catchment and Valley

4.1.1 Basin Geometry

Drainage basin geometry is related to the form or shape of the basin controlled by structure, relief, slope, lithology, and precipitation (Singh 2005). Basin shapes vary from narrow elongated forms to oval and circular. The form factor value will always be 0.7857 for a river basin of compact massive circular shape (Sen 1989). Lower value of the form factor, less than 0.7857, represents a narrow elongated basin area. The values of selected catchments vary from 0.12 to 0.25, depicting an overall elongated nature (Table 3).

The index of shape ratio expresses the extreme elongation for higher values while the lower ones signify circular shape. The shape ratio of the rivers like Jiti, Pagli, Balason, Lish, Rehti, and Mahananda ranges from 2.05 to 2.77. While the values of Gish, Chel, Neora, and Murti are 3.09, 4.8, 3.31, and 4.41 respectively. Only river Diana is an exception, registering a value less than 2. On the other hand, the value

Table 3 Computation of the morphometric indices for the selected river basins

Catchment	Mfs	Form factor	Basin shape factor	Circularity ratio	Elongation ratio	Topographic symmetry factor	Vf ratio	Channel concavity	Mean SL	HI	STD	Relief ratio
Balason	1.92	0.22	2.41	0.33	0.53	0.30	0.15	0.020	106.84	0.28	717.2	0.06
Mahananda	1.52	0.22	2.77	0.28	0.53	0.59	0.1	0.059	164.54	0.22	610.1	0.08
Lish	2.07	0.19	2.44	0.33	0.49	0.50	0.28	0.043	112.42	0.20	508.7	0.09
Gish	1.83	0.19	3.09	0.31	0.49	0.43	0.19	0.027	142.15	0.28	635.4	0.06
Neora	2.01	0.18	3.31	0.23	0.48	0.30	0.28	0.342	170.01	0.15	883.9	0.06
Chel	1.77	0.12	4.80	0.18	0.40	0.26	0.07	0.034	152.36	0.20	675.6	0.06
Murti	1.74	0.14	4.41	0.19	0.42	0.44	0.14	0.035	167.51	0.15	688.3	0.07
Jiti	2.38	0.25	2.05	0.34	0.56	0.31	0.1	0.070	212.21	0.38	911.1	0.13
Diana	2.71	0.16	1.70	0.16	0.45	0.38	0.15	0.044	245.19	0.27	706.1	0.06
Rehti	2.32	0.19	2.47	0.26	0.50	0.44	0.24	0.011	61.22	0.18	486.9	0.05
Pagli	2.170	0.185	2.224	0.255	0.485	0.48	0.15	0.290	93.56	0.100	441.3	0.04

of the Circularity ratio (Rc) varies from 0 to 1, where a lower value indicates an oval or elongated shape. The Circularity ratio of the selected rivers ranges from 0.16 to 0.34, revealing the elongated shape of the drainage basins. Like Rc, the lower value (less than 1) of elongation ratio (Re) also represents the elongated form of the basin, while the values approaching unity will indicate a rounded basin area. Here, the Re varies from 0.4 to 0.53, demonstrating the shape of the basins is invariably oval to elongated. The geometry of the selected drainage basins reflects significantly elongated in shape, which points towards the prosecuted impact of the geologic structure and neotectonics of the concerned region.

4.1.2   Basin Asymmetry

The asymmetric factor of a drainage basin is an important measurement to detect tectonic tilting (Keller and Pinter 2002). When the Transverse Topographic Symmetry Factor (TTSF) is 0, it represents the basin in perfect symmetry, otherwise asymmetric or having a relative tilt towards a particular side. The TTSF, in this study varies between 0.3 and 0.59, indicating the more or less asymmetric character of the basins initiated by surface orogeny. The Balason River on the piedmont surface was found following a fault line lying NNW-SSE along the western flank of the basin. Apart from that formation of the Rakti-Rohini fan surface, covering the interfluve of Balason and Mahananda River has created a local tilt towards the east, governing the development of the path along the eastern margin of the watershed (Fig. 5). Similarly, the development of the blind thrust across the Matiali fan surface has governed a flow deflection for the Chel River towards the west. The elevated terrace surface near Totopara has resulted in a local tilt of the said surface towards the east which has sidetracked the flow of Pagli significantly.

4.1.3   Relief Aspect

Relief aspect of a drainage basin highlights the influence of upliftment and erosional process in modifying the terrain character and its roughness. Relief Ratio (Rr) is a simple statistical tool to characterize the relief properties of a drainage basin (Schumm 1956). High values of the Rr are associated with steep slopes, while a low value indicates a gentler slope having resistant basement rock. Although the Rr values of the concerned catchments vary from 0.04 to 0.13, showing moderate to low relief features, Rr of the mountainous catchment separately, ranges from 0.09 to 0.95. On the HFB region due to the associations of low relief features, the values range between 0.01 and 0.03. Interestingly, Gish river basin has registered maximum Rr on the mountainous part and lowest Rr on the piedmont slope among the selected rivers (Table 4).

The topographic roughness (STD), pointing towards the terrain undulations ranges from 441.36 to 911.10 among the studied catchment. It was found comparatively higher for the river basins like Jiti (911.10) and Neora (833.90), whereas Rehti and
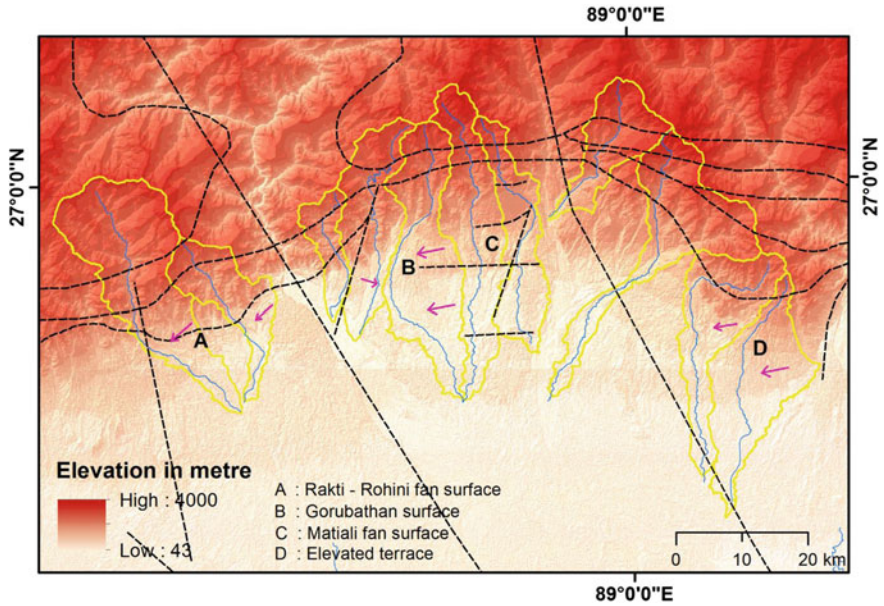
Fig. 5 Characteristic basin tilt within the study area and association of the major deformations and geomorphic units

Table 4 Distribution of the Relief ratio and Hypsometric integral values for the selected catchments on the mountainous part and on the HFB

Catchment	Relief ratio		Hypsometric integral	
	mountain	Piedmont	Mountain	Piedmont
Balason	0.089	0.019	0.50	0.50
Mahananda	0.14	0.014	0.50	0.47
Lish	0.13	0.016	0.49	0.45
Gish	0.95	0.012	0.48	0.49
Neora	0.14	0.02	0.50	0.49
Chel	0.15	0.010	0.50	0.50
Murti	0.18	0.015	0.49	0.45
Jiti	0.17	0.030	0.49	0.49
Diana	0.20	0.01	0.49	0.44
Rehti	0.14	0.01	0.50	0.49
Pagli	0.19	0.013	0.48	0.48

Pagli are sharing the lower values of 486.89 and 441.36 respectively. Higher STD signifies greater elevation anomaly within a concerned spatial extent. Since the STD is calculated as the standard deviation of elevation value from the mean elevation of the catchment, the catchments experiencing comparatively higher STDs illustrate relative skewness in the distribution of elevation values due to differential upliftments.

Valley floor width to height ratio (V_f) is a highly useful geomorphic tool to describe active tectonism. Any value, less than 1 indicates the deep and narrow valley, dominated by active incision associated with active tectonism, whereas a higher value shows the broad valley character, signifying stability. The V_f values of selected river basins range from 0.71 to 0.28, reflecting an overall dominance of incision close to the mountain fronts. Although, the different segments of the rivers were found with differences in intensity of dominance by the upliftment or fluvial action. Moreover, the mountain reaches for most of the rivers are being dominated by active tectonism as the Vf was found significantly lower than 1. On the Quaternary basin-fill segment, the formation of terraces, scarps and debris cones were found invoking valley confinements.

Hypsometric integral (HI) ranges between 0 to 1, where, usually value greater than 0.5 signifies the youthful stage, represents by a convex curve, any value between 0.4 to 0.5 displays a concave-convex slope, disclosing the mature stage. Lastly, any value lower than 0.40 represents the senile stage, showing a concave slope. The HI of the selected river basins varies between 0.47 and 0.51, indicating the basins are in the mature stage and attaining a state of dynamic equilibrium. There has not been any significant difference found while calculating the HI separately on the mountainous catchment and piedmont slope for the selected river basins. It suggests that the rivers are still going through a state of balance between heavy input of sediments that result in aggradation and on the other hand, active orogenic nature leads toward slope deformations (Table 4).

4.1.4 Mountain Front Sinuosity

Mountain front sinuosity (Mfs) was developed to measure the competition between the active surface upliftment and fluvial erosion (Bull 1977). The values of Mountain front sinuosity near to 1 or less than 1.4 usually signifies tectonically active fronts (Keller 1986) and higher than 3 indicates inactive fronts (Bull 2007). The mountain front sinuosity values of the selected rivers in the frontal zone of the Eastern Himalayas varies from 1.52 to 2.71. The SMF values of the rivers namely Balason, Mahananda, Gish, Chel, and Murti are found 1.92, 1.52, 1.83, 1.77, and 1.74 respectively, representing a moderately active frontal zone, while the rest of the rivers like Neora (2.01), Lish (2.07), Pagli (2.17), Jiti (2.38) and Diana (2.71) represent low to the moderate orogenic activity along the mountain front. Since the lesser Himalayan complex is composed of crystalline rocks, fragile to fluvial erosion, the fluvial action continues to perform beside the tectonic upliftment (Fig. 6).
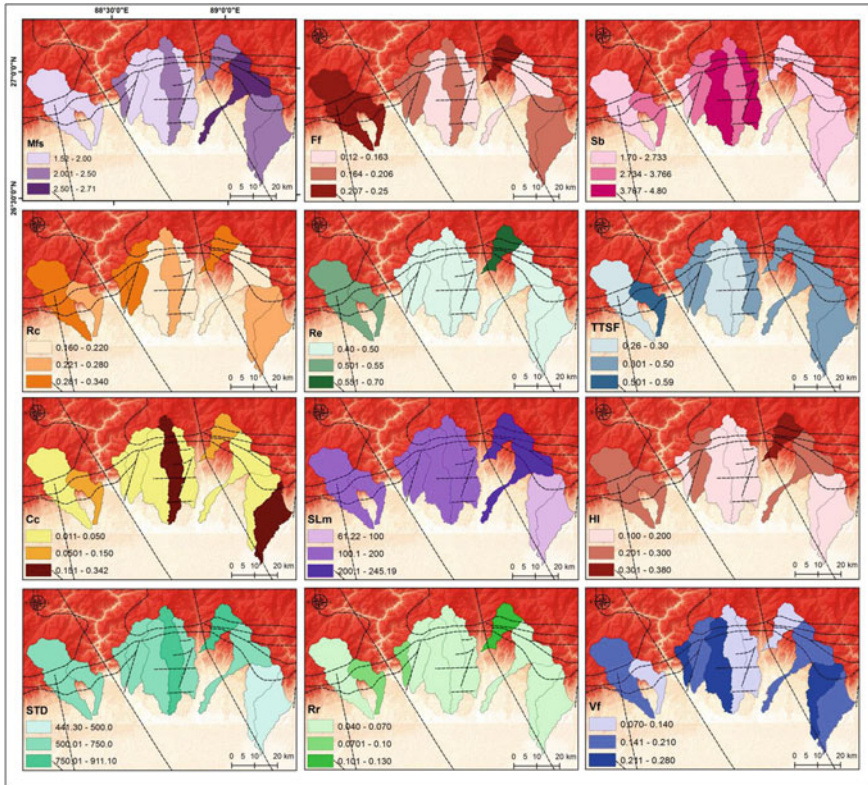
Fig. 6 Spatial representation of the geomorphic indices

4.2 Catchment Scale Adjustment and Localised Abnormalities of Channel Long Profile Forms to Neotectonic Movements

4.2.1 Mathematic Models

The best fit mathematical models for the corresponding normalised long profiles of the rivers has been shown in Table 5. Among the selected eleven rivers, the Mahananda (up to its confluence with Balason) and Pagli River were found best fitted with the logarithmic model. The mathematical curve fitting of the Chel river was the most interesting among all. Although it has registered the best fit with the exponential model but falls marginally separate from the logarithmic model. Except for the above-mentioned rivers, the remaining rivers were found best fitted with an exponential model. Since, the selected rivers although, originate on the mountain terrain but not in association with any large glaciers, not a single river was found fitted best with the power relation. Power relation corresponds to high discharge

Table 5 Curve fitting on the longitudinal profile of the rivers and its statictical significance; cells marked in yellow shows the most significant mathematical model

Rivers	Length	Gradient	No of samples	Coefficient of determination (R²)			
				Linear	Exponential	Logarithmic	Power
Balason	52.065	48.09	202	0.83	0.98	0.82	0.66
Mahananda (up to confluence)	35.706	56.29	136	0.527	0.839	0.93	0.87
Lish	26.783	66.12	106	0.709	0.946	0.86	0.69
Gish	50.244	44.66	198	0.856	0.979	0.75	0.60
Chel	58.856	52.09	221	0.54	0.865	0.861	0.80
Neora	61.391	38.60	248	0.640	0.898	0.76	0.71
Murti	55.764	43.61	222	0.609	0.906	0.87	0.76
Jiti	31.136	103.73	126	0.777	0.964	0.81	0.65
Diana	63.563	38.56	255	0.52	0.87	0.83	0.79
Rehti	57.563	30.50	231	0.789	0.982	0.88	0.71
Pagli	48	32.47	198	0.595	0.888	0.94	0.77

rivers nearly achieving their graded form. The selected rivers are rainfall and run-off fed channels with a flashy discharge character during the dominant monsoon months. Even channel flow in a few of the rivers becomes so feeble that is hard to distinguish during the lean period (Soja and Sarkar 2008). Along with that, also not a single channel was found in correspondence with the linear function asserting the strong influence of surface upliftment and higher intensity of erosion. It is because these rivers are antecedent in nature, thus incised its paths on the lesser Himalayan terrain and the frontal plain segment (Goswami et al. 2012).

4.2.2 Standardised Long Profiles and Mean SL Index

The representation of the longitudinal profile in semi-logarithmic scale was done to characterise the nature of its deviation from the ideal graded profile. The semi-logarithmic profile or the Hack's profile of a river tends to be convex if it experiences surface warping and differential upliftment within its course. The graded profile in a semi-logarithmic scale seems to be a perfectly straight line, decaying downstream (Hack 1973). The convex nature of the profiles plotted on a semi-logarithmic scale signifies the role of active neotectonism and resultant channel slope deformation in the study area (Fig. 7). Stream Length Gradient Index (SL) targets the influence of lithological and tectonic activities that determines the changes in the long profile due to differential bulging of sediments and slope deformations. The current investigation is dealing with the overall SL value for the selected rivers, varying from 61.22 to 245.19. Diana and Jiti display comparatively higher SL values of 245.19 and 212.21
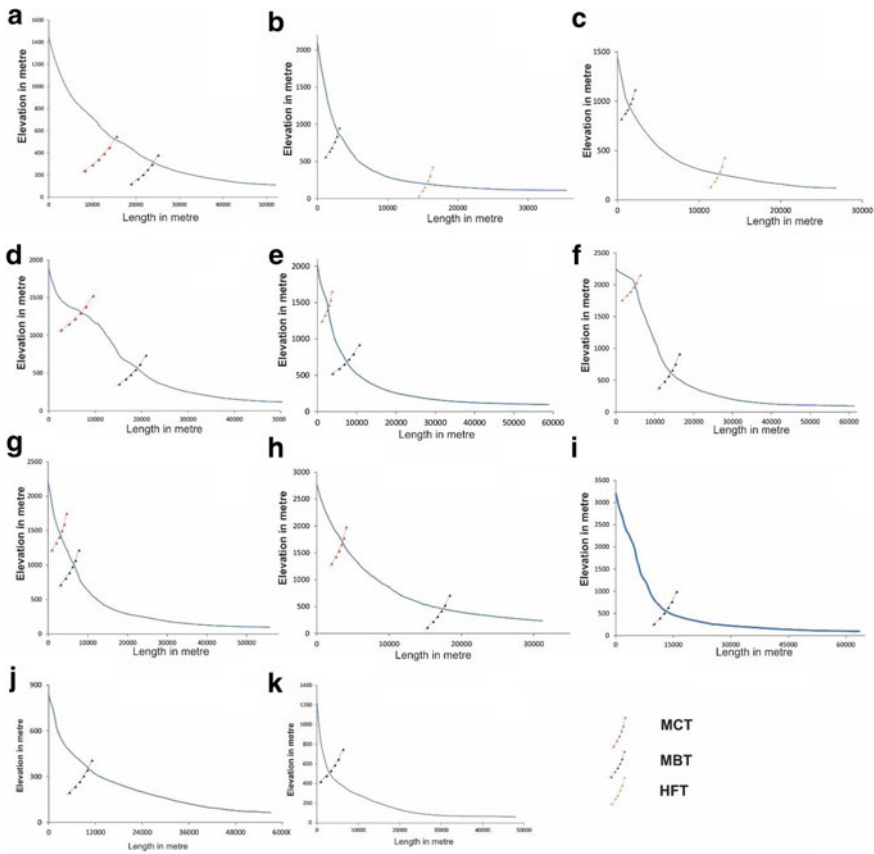
Fig. 7 Semi-logarithmic profiles of the selected rivers. Elevation values were derived from the SRTM 30 m DEM; the sequence of the rivers (in alphabets) is similar to that of mentioned in Fig. 2

respectively. On the other hand, Rehti and Pagli represent the lowest value of SL index among the eleven studied rivers (61.22 and 93.56 respectively). Higher values of average SL (SLm) represents a greater fall in the gradient concerning its watershed margin.

4.2.3 Quantification of the Magnitude of Adjustment: Normalised Gradient Index (NSL)

The segment-specific SL values were divided by the corresponding average SL or the absolute K value to compute the channel steepness or the Normalised Gradient Index (NSL). The values were classified into five separate classes, where NSL < 2 was considered as near flat segments. The intensity of the steepness increases with values above 2, where channel segments with NSL > 10 can be considered as near
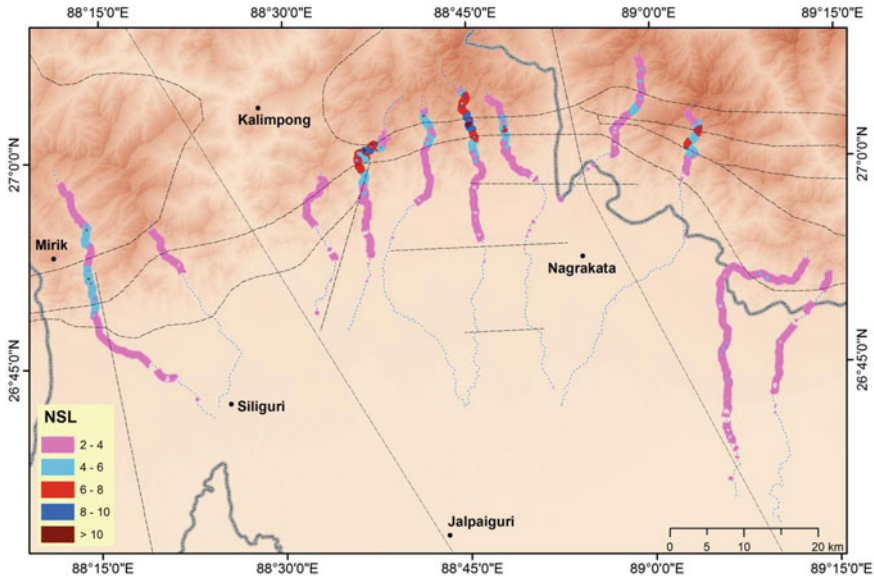
Fig. 8 Interpolation of the Normalised SL or channel steepness values of the selected rivers

vertical fall (Fig. 8). The mountainous reaches of all the rivers were found situated with considerable channel steepness. The reaches associated with the Himalayan thrusts in the Gish, Neora and Diana Rivers were found with maximum steepness and certain near-vertical falls in the river courses. On the alluvial foreland, for natural reasons the steepness went on decreasing in comparison with the mountain reach. Compared to other rivers on the piedmont slope, floe path of Neora and Rehti were found with relatively steeper segments associated with the blind thrusts and uplifted terraces along the neotectonic fault of the Totopara region respectively. Visual observations provide a close association of the relative departures in channel steepness along the Himalayan thrusts invariably for all the selected river courses. The average channel steepness was found interesting. Balason, Gish, Neora, Jiti and Rehti river has maintained an overall steep profile with local departures. On the other hand, Lish was found marginally on the steeper side with an overall steepness of 2.08. Diana river was observed with major departures in the relative steepness of the profile but overall it was found as a near flat river course since, on the piedmont, lesser confinements and lower degrees of disturbances in terms of endogenetic perturbations has led to developing a near flat middle to lower reach (Table 6).

4.2.4 Quantifying the Localised Anomalies; RDet Index

The Rdet index identifies the major slope anomalies in the river long profiles (Moussi et al. 2018). In this study, the Rdet has been portrayed in three different ways; one, extracting the major breaks at an interval of 100 m, starting from 200 m. It was started

Table 6 General statistics of the Normalised SL values for the selected river basins

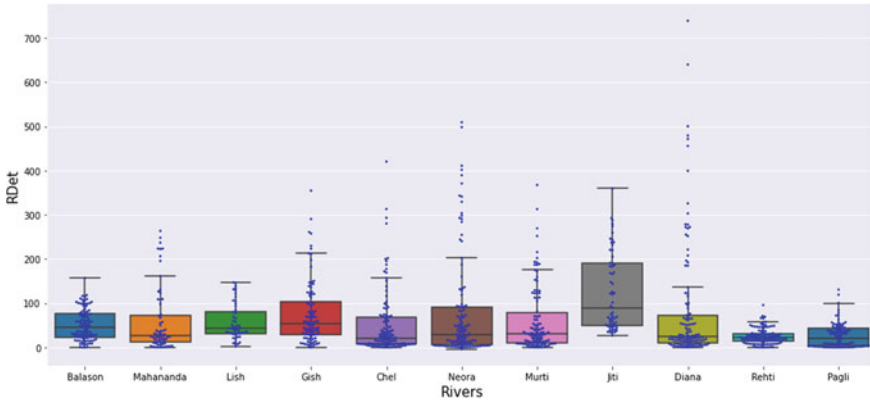|	Balason	Mahananda	Lish	Gish	Chel	Neora	Murti	Jiti	Diana	Rehti	Pagli
Mean	3.44	3.09	2.75	4.567	3.344	4.712	3.433	3.259	4.324	3.036	2.474
Max	6.77	4.184	3.86	13.58	6.906	13.42	8.167	5.747	9.273	4.907	3.411
Min	2.16	1.678	2.05	2.036	2.015	1.412	2.067	1.736	2.138	1.327	2.003
St Dev	1.13	0.75	0.55	2.46	1.14	2.66	1.29	0.93	2.09	0.67	0.34
CV	32.8	24.38	20.06	53.94	34.21	56.61	37.86	28.75	48.38	22.18	13.85

Fig. 9   River respective categorical distribution of the Rdet values

from 200 m because values less than 200 were found too ubiquitous to consider as an anomaly. Second, Rdet values computed at the random interval was interpolated using the IDW module in Arc-GIS and third, the categorical distribution of Rdet values within the major tectono-geomorphic domains of the Himalayas and the associated Quaternary alluvial fill basin. These perspectives add up cartography with simplified visualisation of the anomaly zones.

The Rdet values of the trunk streams of eleven selected basins have been illustrated in Fig. 9 where the highest value was found 764 m in the Diana River, around a segment associated with thrust faults. The river respective categorical distribution of the Rdet values portrays a non-uniform distributional scenario among the selected rivers. The distribution was found less skewed for Balason, Lish and Jiti River where no outliers were found. The distribution of the outliers depicts the issue of an anomaly in the slope of the river courses. It is evident in river courses like Diana, Chel and Neora where extreme outliers signify greater anomalies and the formation of major breaks in the longitudinal slope. The spatial distribution of the interpolated Rdet (Fig. 10) shows the exact locations of the outliers in the courses of Mahananda, Gish, Chel, Neora, Murti and Diana. In most of the state, the anomalous zone or the knick zones are associated with the thrust faults lying into the domain of lesser Himalayan complex (Fig. 11). The distribution of the Rdet values in the Greater Himalayan complex was found less anomalous compared to the lesser Himalayan complex (Fig. 12). Except in the course of Jiti and Neora, no other rivers have significantly registered anomalous values in the Greater Himalayan domain. Apart from that, the Siwalik pockets were found with lesser disturbances with comparatively lower skewness but the associated foreland region was found with greater anomalies. Except for an abrupt break in the Neora River at the junction of the mountains and plains, registering a Rdet value above 200 m, no other anomaly of considered intensity was found on the HFB in any of the river courses. Compared to the spatial distribution, the zone respective categorical distribution has outlined multiple anomalies on the forelabd domain. Thus, the spatiality of the Rdet on the HFB was studied
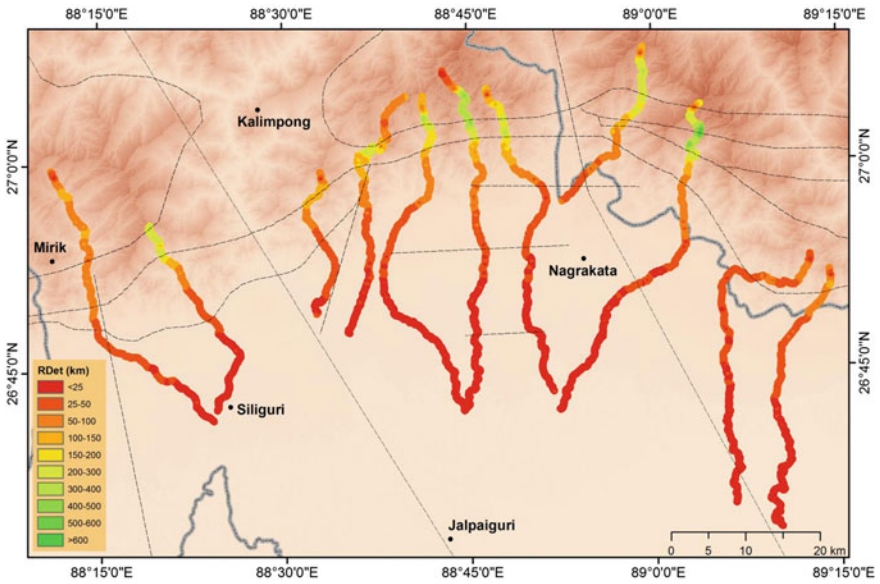
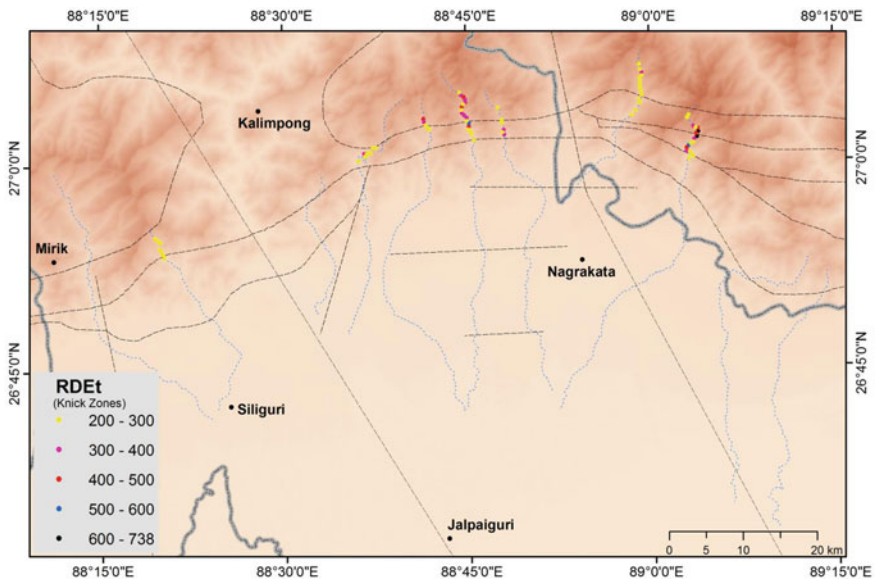**Fig. 10** Interpolation of the RDet values of the selected rivers

Fig. 11 Knick zones found in the study area. The values were selected based on a certain interval, starting from 200 m
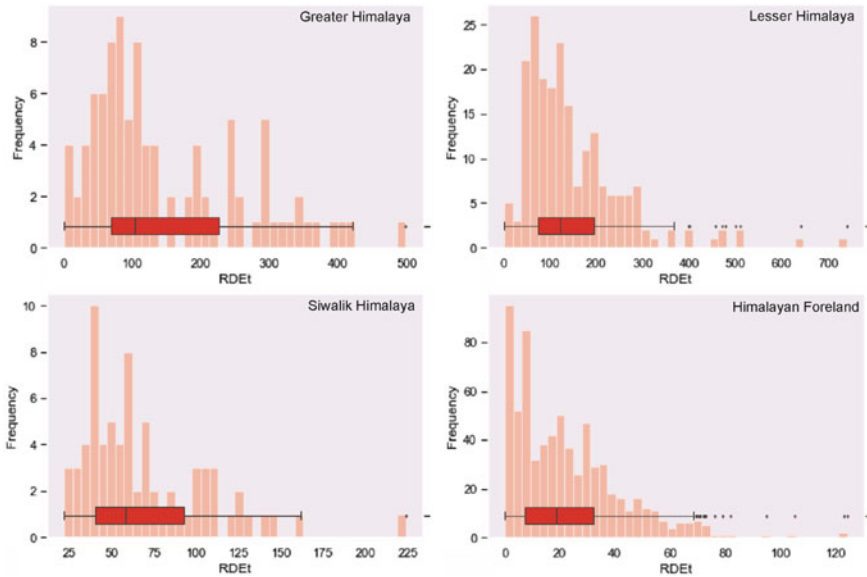
Fig. 12 Distribution of the Rdet values within distinct tectonogeomorphic zones in the study area. The outliers were considered as the slope anomaly in the river reaches

separately and the anomalous condition was mapped based on the boundary of its upper whisker (Fig. 13). Around the mountain front, the anomalous condition was found in rivers like Chel, Neora, Murti, Diana and Pagli. Among these five channels, the anomalous condition in Neora and Murti was found associated with the Matiali scarp (blind thrust) while a similar issue of slope anomaly was also associated in the Pagli River at intersection of the neotectonic fault. Since all the rivers has been originated on the Higher or Lesser Himalayas, these are antecedent to the faults. The abrupt surface warping had created an anomalous condition in the long profiles as the rivers continued to down cut during the surface upliftment.

4.3 Overview of Channel Responses to Neotectonic Perturbations

The geospatial approach applied in this study has helped to derive the nature of fluvial responses, collectively at the catchment form to its evolution phases through adjusting its longitudinal forms. The catchment forms have significantly portrayed confinity effects in its development which is usually governed by the tectonic perturbations that result in basin elongation (Bull and McFadden 1987). Surface warping and tectonism led surface deformations often create relief barriers for rivers. It is most common in the form of ridges that compel a river to deviate either due to physical contact or
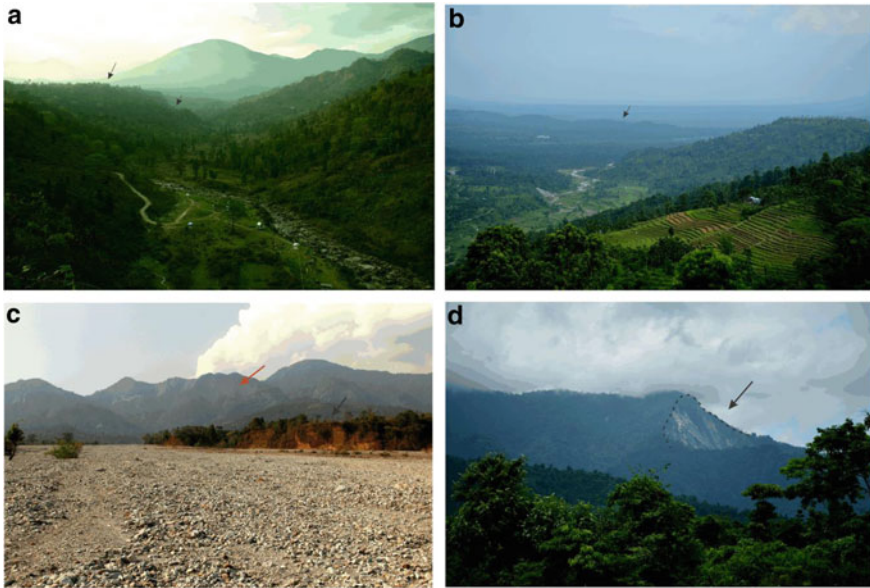
Fig. 13 **a** Unpaired terraces along the course of Murti River (viewing upstream); **b** Chasla scarp lying parallel to the mountain front (viewing downstream); **c** Uplifted terrace surface (Totopara surface) with exposed faultscarp of a neotectonic fault located on the east of Pagli River (viewing west); **d** Triangular facets developed around fault scarp near Pagli River (viewing north)

surface tilt through surface slope modification (Holbrook and Schumm 1999). The results of basin asymmetry of the selected river basins show significant tilting at varied directions but are found immediately associated with structural elements. Although the regional tilt on the eastern side of the Teesta river is towards SE but the effective local deformations concentrated at a certain part, have resulted in the basin tilting in varied directions. Here, the impact of the alluvial fan attitude cannot be overruled. It has significantly governed the channel direction around the mountain front as well as on the piedmonts (Chakraborty and Mukhopadhyay 2013). Similar findings were also encountered by Sharma and Sarma (2017) within the belt of Schuppen where local deformations have produced tilts in varied directions. At the mountain piedmont junctions, cessation of upliftment allows fluvial action to dominate which results into transformation of the linear and active mountain fronts into a zig-zag form. Although it requires less resistant lithological composition. In any intermediate state of action, upliftment and fluvial erosion go hand in hand (Bull 2007). Similarly, upliftment of the tectonically active frontal surface attracts intense downcutting, resulting into deeply incised valleys (Bull and McFadden 1977; Bull 2007). In this study, mountain fronts of the river basins seemed to be moderate to low tectonically active but still present with incised river valleys as a portrayal of ongoing upliftment. The less resistant lithological composition around the frontal part of the Himalayan complex allowed fluvial erosion to change the linearity of the front. The imprints

of simultaneously active Himalayan upliftment are also quite distinct as observed through Vf ratio which is invariably < 1 for all the selected courses around the corresponding mountain fronts. Thus, the process of Himalayan upliftment is neither dormant or rigorous along its frontal segment within the studied part.

Besides the location of structural elements, rock erodibility or certain litho-contacts and differential upliftment can also influence the essential drop in down-stream channel slope (Troiani et al. 2014; Pavano et al. 2016; Moussi et al. 2018). The Himalayan complex, contemplated with multiple thrusts and intra-formational thrust sheets were found as the major zones of concentration of slope anomalies or knick points. Although the nature of concentration has varied throughout the extent. The formation of the knickpoints suggests differential upliftment of the surface where reconstruction of the river flow paths gets fragmented into multiple phases in response to these perturbations. The differential upliftment was within the Spiti River basin in the Westen Himalaya was found associated with spatially varying concentrations and intensity of breaks in the channel longitudinal slope (Phartiyal and Kothyari 2011). Apart from the spatial distribution of the knick points, for inferring the lithological and surface material composition on the knickpoints, it was categorically grouped interms of different tectono-geomorphic domains in the study area. The associa-tion of the anomalous zone was invariably concentrated into the zone with relatively highest density of the thrust faults or simpler to say, the region with maximum surface deformations due to faulting. The enclosed region of the MCT and MBT around the apex of the reentrant has been found with relatively higher values of NSL compared to other segments with a dominance of knickpoint clusters. Thus, it is being infered that the higher rate of upliftment of the MCT and associated channel incision in order to adjust the upliftment pace has resulted in greater intensity of long profile deformation. The rate might have varied through out the extent. Apart from that, the topographic barriers of the Himalayas attracts greater railfall which might have been another potential agent ignited the rapid incision compared to other topographic extents. Although the frontal part of the Himalayas acts as orographic front that helps in monsoon orography and a major difference in rainfall intensity usually found over the Greater Himalayas compared to the Middle Himalayas (Rees and Collins 2006). Moreover, the summer monsoon gets weaker as it moves towards west along the Himalayan front and a clear distinction can be made on the east and western part of Teesta. Thus, strengthening the rainfall intensity results in active erosion that perhaps influence the isostatic upliftment or tectonic upliftment (Bishop et al. 2002). These differential upliftment along between the MBT and MCT and continuing growth process of the intra-formational thrust sheets in this region has resulted in adjust-ment of the river long profile forms to surface ruptures. Here, we infer that since, the lithological composition of the Himalayan segment being analysed in this study are present with no such major distinguished variations in lithology, the tectonic impact and differential surface warping has compelled the fluvial system to adjust accordingly and resulted into major slope anomalies formed whenever scarps and fault lines were encountered.

5   Conclusion

The morphotectonic approach applied on a selected segment of the Eastern Himalayas has revealed a mutual association of fluvial action and epirogenic activity where the rivers are mostly anteceedent to the recent developments of structural elements. Thus, the ongoing incision in order to accommodate the uplift is characteristic outcome of such association. The neotectonic activeness of the Quaternary alluvial fill basin of the foreland part has been significantly associated with flow paths of the trunk streams to the development of the landscape features. The overall tectonogeomorphic environment has significantly impacted the evolution of the fluvial systems, starting from its basin planimetric properties to valley form as well as longitudinal slope. The morphometric data has inferred that these basins are tilted, highly asymmetric, thoroughly confined to get the elongated form and tectonically deformed which have attracted terrain roughness to slope anomalies both a catchment scale and valley forms. Although, invariably for most of the rivers, the intensity of slope fall and deformation on the river longitudinal forms are found highly associated with the location of the Himalayan Thrusts but the dominance of the knick points on the mountainous tract is present around the apex of the reentrant. On the other hand, the channel slope deformation on the piedmont slope is significantly associated with neotectonic twitchings in case of Gish, Chel, Neora, Murti, Rehti and Pagli River (Fig. 13). Compared to all, channels located around the apex and eastern flank of the reentrant are more deformaed due to the formation of sub-parallel thrusts to the Himalayan thrusts, translational thrust sheets and neotectonic scarps. The uniqueness of this work lies on the process-response approach, commenced to study the tectonic indentations and corresponding geomorphic responses at catchment scale to channel longitudinal form.

References

Altın BT (2012) Geomorphic signatures of active tectonic in drainage basins in the Southern Bolkar mountain, Turkey. J Indian Soc Remote Sens 40(2):271–285. https://doi.org/10.1007/s12524-011-0145-8

Ayaz S, Dhali MDK (2019) Longitudinal profiles and geomorphic indices analysis on tectonic evidence of fluvial form, process and landform deformation of Eastern Himalayan Rivers, India. Geol Ecol Landscapes 4(1):11–22. https://doi.org/10.1080/24749508.2019.1568130

Ayaz S, Biswas M, Dhali MK (2018) Morphotectonic analysis of alluvial fan dynamics: comparative study in spatio-temporal scale of Himalayan foothill. India. Arabian J Geosci 11:41. https://doi.org/10.1007/s12517-017-3308-2

Bali BS, Wani AA, Khan RA, Ahmad S (2016) Morphotectonic analysis of the Madhumati watershed, northeast Kashmir Valley. Arabian J Geosci 9:390. https://doi.org/10.1007/s12517-016-2395-9

Bhattacharyya K, Mitra G (2011) Strain softening along the MCT zone from the Sikkim Himalaya: Relative roles of Quartz and Micas. J Struct Geol 33:1105–1121. https://doi.org/10.1016/j.jsg.2011.03.008

Bishop MP, Shroder Jr JF, Bonk R, Olsenholler J (2002) Geomorphic change in high mountains: a western Himalayan perspective. Global Planet Change 32:311–329

Bull WB, McFadden LD (1977) Tectonic geomorphology North and South Garlock fault, California. Eight annual geomorpholofy symposium, State University of New York, (pp. 115–138). Binghamton

Bull W (2007) Tectonic geomorphology of mountains: a new approach to paleoseismology. Wiley-Blackwell, Oxford, p 328

Burbank DW, Anderson RS (2012) Tectonic geomorphology. Blackwell publishing Ltd

Burbank D, Leland J, Fielding E et al (1996) Bedrock incision, rock uplift and threshold hillslopes in the northwestern Himalayas. Nature 379:505–510. https://doi.org/10.1038/379505a0

Chakraborty PP, Tandon SK, Roy SB, Saha S, Paul PP (2020) Proterozoic sedimentary basins of India. Switzerland AG: Springer Geology. https://doi.org/10.1007/978-3-030-15989-4

Chatterjee RS, Nath S, Kumar SG (2019) Morphotectonic analysis of the Himalayan Frontal region of Northwest Himalaya in the light of geomorphic signatures of active tectonics. Singapore: Springer Nature

Chen YC, Sung Q, Chen CN, Jean JS (2006) Variations in tectonic activities of the central and southwesternfoothills, Taiwan, inferred from river Hack profiles. Terrestrial, Atmosph Oceanic Sci 17:563–578

Cox RT (1994) Analysis of drainage basins symmetry as rapid tecnique to identify areas of possible quaternary tilt-block tectonics: an example from Mississippi Embayment. Geol Soc Am Bull 106:571–581

Dasgupta S, Mukhopadhyay B, Mukhopadhyay M, Nandy D (2013) Role of transverse tectonics in the Himalayan collision: further evidences from two contemporary earthquakes. J Geol Soc India 81:241–247

DeCelles Peter G, Giles Katherine A (1996) Foreland basin systems. Basin Res 8(2):105–123. https://doi.org/10.1046/j.1365-2117.1996.01491.x

Dubey RK, Satyam GP (2018) Morphotectonic appraisal of Yamuna river basin in headwater region: a relative active tectonics purview. Geological Soc India 92:346–356. https://doi.org/10.1007/s12594-018-1018-3

Figueiredo PM, Rockwell TK, Cabral J, Ponte LC (2017) Morphotectonics in a low tectonic rate area: analysis of the southern Portuguese Atlantic coastal region. Geomorphology. https://doi.org/10.1016/j.geomorph.2018.02.019

Flores-Prieto, E., Quénéhervé, G., Bachofer, F., Shahzad, F., & Maerker, M. (2015). Morphotectonic Interpretation of the Makuyuni Catchment in Northern Tanzania using DEM and SAR data. Geomorphology. https://doi.org/10.1016/j.geomorph.2015.07.049

Gansser A (1964) Geology of himalayas. Interscience publishers, New York

Ghosh S, Sivakumar R (2018) Assessment of morphometric parameters for the development of relative active tectonic index and its significant for seismic hazard study: an integrated geoinformatic approach. Environ Earth Sci 77:600. https://doi.org/10.1007/s12665-018-7787-6

Goswami C, Mukhopadhyay D, Poddar BC (2012) Tectonic control on the drainage system in a piedmont region in tectonically active Eastern Himalayas. Frontiers Earth Sci 6(1):29–38. https://doi.org/10.1007/s11707-012-0297-z

Goswami PK, Pant CC (2008) Tectonic evolution of Duns in Kumaun sub-Himalaya, India: a remote sensing and GIS based study. Int J Remote Sens 29(16):4721–4734

Guha D, Bardhan S, Basir SR, De AK, Sarkar A (2007) Imprints of Himalayan thrust tectonics on the Quaternary piedmont sediments of the Neora-Jaldhaka Valley, Darjeeling-Sikkim Sub-Himalayas, India. J Asian Earth Sci 30:464–473. https://doi.org/10.1016/j.jseaes.2006.11.010

Hack JT (1957) Studies of longitudinal river profiles in Virginia and Maryland. U.S. Geological Survey Professional Paper (pp 249B-99)

Hack JT (1973) Stream-profile analysis and stream-gradient index. J Res U.S. Geol Surv 1(4):421–429

Hawker LP, Rougier J, Neal J, Bates P, Archer L, Yamazaki D, (2018) Implications of simulating global digital elevation models for flood inundation studies. Water Res 54:7910–7928. https://doi.org/10.1029/2018wr023279

Holbrook J, Schumm SA (1999) Geomorphic and sedimentary response of rivers to tectonic deformation: a brief review and critique of the tools for recognizing subtle epeirogenic deformation in modern and ancient settings. Tectonophysics 305:287–306

Jain V, Sinha R (2005) Response of active tectonics on the alluvial Baghmati River, Himalayan foreland basin, eastern India. Geomorphology 70:339–356. https://doi.org/10.1016/j.geomorph.2005.02.012

Joshi LM, Pant PD, Kotlia BS, Kothyari GC, Luirei K, Singh AK (2016) Structural overview and morphotectonic evolution of a strike-slip fault in the zone of North Almora Thrust, Central Kumaun Himalaya, India. J Geol Res, 16. https://doi.org/10.1155/2016/6980943

Kale VS, Sengupta S, Achyuthan H, Jaiswal MK (2013) Tectonic controls upon Kaveri river drainage, Cratonic Peninsular India: inferences from longitudinal profiles, morphotectonic indices, hanging valleys and fluvial records. Gromorphology.https://doi.org/10.1016/j.geomorph.2013.07.027

Kar R, Chakraborty T (2014) Comment on "Geomorphology in relation to tectonics: A case study from the eastern Himalayan foothills of West Bengal, India" by Chandreyee Chakrabarti Goswami, Dhruba Mukhopadhyay, B. C. Poddar [Quaternary International, 298, 80e92]. Quatern Int 338:113–118. https://doi.org/10.1016/j.quaint.2014.01.041

Kashani R, Partabian A, Nourbakhsh A (2009) Tectonic implication of geomorphometric analyses along the Saravan Fault: evidence of a difference in tectonic movements between the Sistan Suture Zone and Makran Mountain Belt. J Mt Sci 16(5):1023–1034

Kaushal RK, Singh V, Mukul M, Jain V (2017) Identification of deformation variability and active structures using geomorphic markers in the Nahan salient, NW Himalaya, India. Quat Int, 1–17. https://doi.org/10.1016/j.quaint.2017.08.015

Keller E, Printer N (1996) Active tectonics: earthquakes, uplift and landscape. Prentics Hall, New Jersey

Keller E, Printer N (2002) Active tectonics: earthquakes, uplift and landscape. Prentice Hall, New Jersey

Klinkenberg B (1992) Fractals and morphometric measures: is there a relationship? Geomorphology 5:5–20

Lave J, Avouca JP (2000) Active folding of fluvial terraces across the Siwalik Hills, Himalaya of Central Nepal. J Geogr Res 105(B3):5735–5770

Lee C-S, Tsai LL (2010) A quantitative analysis for geomorphic indices of longitudinal river profile: a case study of the Choushui River, Central Taiwan. Environ Earth Sci 59:1549–1558. https://doi.org/10.1007/s12665-009-0140-3

Lu P, Shang Y (2015) Active tectonics revealed by river profiles along the Puqu fault. Water 7:1628–1648. https://doi.org/10.3390/w7041628

Malik JN, Mohanty C (2007) Active tectonic influence on the evolution of drainage and landscape: Geomorphic signatures from frontal and hinterland areas along the Northwestern Himalaya, India. J Asian Earth Sci 29:604–618. https://doi.org/10.1016/j.jseaes.2006.03.010

Mallet FR (1875) On the geology and mineral resources of the Darjiling district and western Duars. Geol Surv India Memoirs 11(1):1–50

Moussi A, Rebail N, Chaieb A, Saadi A (2018) GIS-based analysis of the stream length-gradient index for evaluating effects of active tectonics:a case study of Enfidha (North-East of Tunisia). Arab J Geosci 11:123. https://doi.org/10.1007/s12517-018-3466-x

Mukul M, Sridevi SJ, Ansari K, Abdul AM (2014) Seismotectonic implications of Strike-slip earthquakes in the Darjiling-Sikkim Himalaya. Curr Sci 106:198–210

Nakata T (1989) Active faults of the Himalaya of India and Nepal. Geol Soc Ameraica Special Paper 232:243–264

Pant CC, Singh SP (2017) Morphotectonic analysis of Kosi river basin in Kumaun Lesser Himalaya: an evidence of neotectonics. Arab J Geosci 10:421. https://doi.org/10.1007/s12517-017-3213-8

Partabian A, Nourbakhsh A, Ameri S (2016) GIS-based evaluation of geomorphic response to tectonic activity in Makran Mountain Range, SE of Iran. Geosci J

Pavano F, Pazzaglia FJ, Catalano S (2016). Knickpoints as geomorphic markers of active tectonics: a case study from northeastern Sicily (southern Italy). Geol Soc America. https://doi.org/10.1130/L577.1

Pérez-Peña JV, Azor A, Azañón JM, Keller EA (2010) Active tectonics in the Sierra Nevada (Betic Cordillera, SE Spain): insights from geomorphic indexes and drainage pattern analysis. Geomorphology, 74–87. https://doi.org/10.1016/j.geomorph.2010.02.020

Phartiyal B, Kothyari GC (2011) Impact of neotectonics on drainage network evolution reconstructed from morphometric indices: case study from NW Indian Himalaya. Z Geomorphol 56(1):121–140. https://doi.org/10.1127/0372-8854/2011/0059

Philip G, Virdi NS, Suresh N (2009) Morphotectonic evolution of Parduni basin: an intradun Piggyback basin in Western Doon Valley, NW outer Himalaya. J Geol Soc India 74:189–199. https://doi.org/10.1007/s12594-009-0121-x

Rees GH, Collins DN (2006) Regional differences in response of flow in glacier-fed Himalayan rivers to climatic warming 20(10):2157–2169

Rhea S (1993) Geomorphic observation of rivers in the Oregon coast range from a regional reconnaissance perspective. Geomorphology 6(2):135–150

Schumm SA (1956) The evolution of drainage systems and slopes in bad lands at Perth, Amboi, New Jersey. GeolSocAme Bull 67 (5):597–646

Schumm (1986) Alluvial river response to active tectonics. In: N.R. Council (ed) Active tectonics. National Academy Press, Washington (D.C.), pp 80–94

Seeber L, Gornitz V (1981) River profiles along the Himalayan arc as indicators of active tectonic. Tectonophysics 92:335–367

Sharma G, Ray PK, Mohanty S (2017) Morphotectonic analysis and GNSS observations for assessment of relative tectonic activity in Alaknanda basin of Garhwal Himalaya, India. Geomorphology

Sharma S, Sarma JN (2017) Application of drainage basin morphotectonic analysis for assessment of tectonic activities over two regional structures of the Northeast India. J Geol Soc India 89:271–280

Singh V, Tandon SK (2008) The Pinjaur dun (intermontane longitudinal valley) and associated active mountain fronts, NW Himalaya: tectonic geomorphology and morphotectonic evolution. Geomorphology 102:376–394. https://doi.org/10.1016/j.geomorph.2008.04.008

Sinha SK, Parker G (1996) Causes of concavity in longitudinal profiles of rivers. Water Resour Res 32:1417–1428

Soja R, Sarkar S (2008) Characteristics of hydrological regime. In: Starkel L, Sarkar S, Soja R, Prokop P (eds), Present-day Evolution of Sikkimese-Bhuta¬nese Himalayan Piedmont (pp 37–46). Warszawa: Stanisława Leszczyckiego

Starkel L, Sarkar S, Prokop P (2008) Present-day evolution of the Sikkimese-Bhutanese Himalayan Piedmont,. PolskaAkademiaNauk, Instytut Geografii IPezestrzennego Zagospodarowania

Summerfield MA (1991) Global geomorphology: an introduction to the study of landforms development. Longman, Harlow

Troiani F, Galve JP, Piacentini D, Seta MD, Guerrero J (2014) Spatial analysis of stream length-gradient (SL) index for detecting hillslope processes: a case of the Gállego River headwaters (Central Pyrenees, Spain). Geomorphology 214:183–197. https://doi.org/10.1016/j.geomorph.2014.02.004

Valdiya KS (2002) Emergence and evolution of Himalaya: reconstructing history in the light of recent studies. Prog Phys Geogr 26(3):360–399

Valdiya KS (1986). Neotectonic activities in the Himalayan belt. New tectonics in South Asia, Surv., (pp 241–267). Dehradun

Valdiya KS, Joshi DD, Sanwal RS, Tandon SK (1984) Geomorphologic development across the active Main Boundary Thrust: an example from the Nainital Hills in Kumaun Himalaya. J Geol Soc India 25:761–774

Virdi NS, Philip G, Bhattacharya S (2007) Neotectonic activity in the Markanda and Bata river basins, Himachal Pradesh, NW Himalaya: a morphotectonic approach. Int J Remote Sens 27(10):2093–2099. https://doi.org/10.1080/01431160500445316

Yin A (2006) Cenozoic tectonic evolution of the Himalayan orogen as constrained by along-strike variation of structural geometry, exhumation history, and foreland sedimentation. Earth-Sci Rev 76:1–131